

# OPTIMIZING CURRENT DENSITY MEASUREMENTS FOR INTENSE LOW BETA ELECTRON BEAMS\*

M. R. Howard<sup>†</sup>, J. E. Coleman, Los Alamos National Laboratory, Los Alamos, NM, U.S.A  
 S. Lidia, Facility for Rare Isotope Beams, Michigan State University, East Lansing, MI, U.S.A

## Abstract

The Cathode Test Stand at LANL is utilized to test velvet emitters over pulse durations of up to 2.5  $\mu$ m. Diode voltages range from 120 kV to 275 kV and extracted currents exceed 25 A and depend on cathode size and pulse duration. Current density measurements taken with scintillators or Cherenkov emitters produce inconsistent patterns that disagree with the anticipated beam profile. Several factors contribute to the measured beam distribution, such as electron scatter, X-ray scatter, and Snell's law. Here, we present a range of experiments designed to evaluate both electron scatter and Cherenkov emission limits in efforts to optimize current density measurements. For electron ranging studies, metal foils of different densities and thicknesses are coupled with a scintillator, which is then imaged with an ICCD. Similarly, Cherenkov emission and Snell's law are investigated through imaging materials with differing indices of refraction over a range of beam energies. MCNP6® modeling is utilized to further guide and evaluate these experimental measurements.

## BACKGROUND AND INTRODUCTION

Beam current density measurements are crucial diagnostics for evaluating particle injectors and can take various forms. Common examples of destructive or invasive diagnostics include fluorescent screens [1], optical transition radiation (OTR) [2], and Cherenkov emitters [3, 4]. When measuring the profile of intense, high-current beams, the diagnostic must be chosen carefully.

Reference [1] utilized a 0.1 mm-thick YAG:Ce scintillator crystal partnered with a 0.025 mm-thick stainless steel foil. Nominal parameters were a 120kV electron beam with a current of 20 A. The foil was used to prevent damage to the scintillation screen and generated a bremsstrahlung X-ray beam which was subsequently imaged on the YAG:Ce. However, this method leads to X-ray scatter within both the foil and the scintillator resulting in a blurred image.

Cherenkov emitters are an alternative diagnostic method and is thought to be preferable as these materials are typically free of fluorescence and subsequent issues [3]. Silica has proven an optimal diagnostic for beams produced via explosive emission [4, 5]. However, Cherenkov emitters must be chosen with caution and the energy thresholds should compliment that of the electron beam.

We discuss challenges with measuring current density for a low-beta ( $\beta < 0.75$ ) electron beam produced from a velvet

cathode and our efforts to optimize this measurement. We describe various experiments and introduce complementary models that characterize the effects believed to construe optical measurements, electron scatter, X-ray scatter, Cherenkov emission, and total internal reflection. These measurements are dependent on material, beam energy, and extracted beam current.

## EXPERIMENTAL DESIGN

All experiments shown were generated with the Cathode Test Stand (CTS) utilizing a velvet cathode. Design goals of the CTS include full documentation of long pulse electron beams from velvet cathodes with a maximum pulse duration of 2.2  $\mu$ s. The AK gap is held constant at 22 mm with an additional emitter recess of 3 mm into the cathode shroud. The emitter size is variable and can range from 7.5 mm to 25 mm in diameter. Diode voltages range from 120 kV to 275 kV, corresponding to  $\gamma = 1.2\text{--}1.5$  and  $\beta = 0.5\text{--}0.75$ . Current measurements are taken after the anode aperture. More details on the diode design can be found in Ref. [6].

The current density diagnostic screen is located 143 mm from the polished stainless steel cathode shroud and is imaged with an intensified fast gated charge-coupled device (ICCD) mounted externally [7]. The camera has a 1024x1024 imaging array with 12.8 x 12.8  $\mu$ m pixels and a 3 ns minimum gate width.

Patterns on the current density diagnostic are highly variable and irregular. The major contributors to this distribution include: electron scatter, X-ray scatter, Cherenkov thresholds, and total internal reflection. Figure 1 shows the current density distribution measured with a BC-400 scintillator coupled with a 100  $\mu$ m-thick piece of aluminum foil. This image corresponded to a beam energy of 235 kV, current of 165 A, and was generated with a 15 mm diameter cathode. The measured beam profile distribution does not represent what is expected and crucial information such as current density or beam radius cannot be extracted due to the irregular pattern. Extracting this information is further complicated by extreme shot-to-shot variability.

## ELECTRON RANGING STUDIES

Metal foils of various Z are placed on the upstream side of the scintillation screen to range out the electrons. The concept, which mirrors that of Ref. [1], is to range out the electrons and image the produced bremsstrahlung X-ray pulse. The distribution will still be affected by X-ray scatter. However, by removing the element of electron scatter, the measured distribution better resembles the expected beam profile.

\* Work supported by Triad National Security, LLC for the National Nuclear Security Administration of U.S. Department of Energy under contract 89233218CNA000001.

<sup>†</sup> mrohoward@lanl.gov

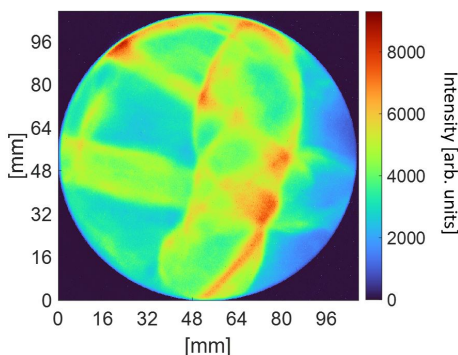


Figure 1: Current density distribution produced with a 15 mm-diameter cathode and a 500  $\mu\text{m}$ -thick BC-400 diagnostic with 100  $\mu\text{m}$ -thick aluminum foil placed upstream. Image taken over 3 ns with  $V = 235$  kV and  $I = 165$  A. (Shot 7247)

Candidate materials were chosen such that electrons were mostly ranged out at the highest obtainable energy. The electron range in Copper ( $Z = 29$ ) for 300 kV electrons is approximately 140  $\mu\text{m}$ . Figure 2 shows a beam distribution with the following material configuration: 200  $\mu\text{m}$ -thick copper foil upstream of a 700  $\mu\text{m}$ -thick plastic BC-400 scintillator. It is evident that issues from electron scatter have been mitigated, and the shot-to-shot variability is drastically improved.

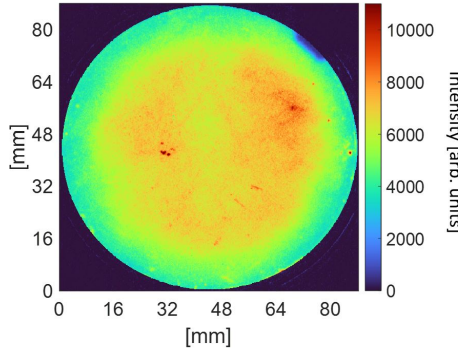


Figure 2: Current density distribution produced with a 15 mm-diameter cathode and a 700  $\mu\text{m}$ -thick BC-400 diagnostic coupled with 200  $\mu\text{m}$ -thick Cu foil where  $V = 229$  kV and  $I = 139$  A. Image taken over 10 ns. (Shot 7798)

## CHERENKOV EMISSION STUDIES

Materials with a wide range of indices of refraction were considered for Cherenkov threshold testing. Ultimately, large suites of data were collected with  $\text{Al}_2\text{O}_3$  and  $\text{SiO}_2$ . These candidates allow for interesting comparisons due to the difference in Cherenkov thresholds. Table 1 lists the index of refraction, Cherenkov energy threshold, and the energy threshold for total internal reflection (TIR) for each material. The CTS does not produce a consistent reliable beam until  $V_{\text{max}} = 180$  kV. For silica, Cherenkov radiation

does not initiate until 190 kV allowing for experiments that can fully diagnose effect from Cherenkov emission. The total internal reflection threshold for this material is not hit until over 900 kV, which is far above the capabilities of the CTS. On the other hand, alumina has a larger index of refraction resulting in a lower threshold of 108 kV and a TIR threshold of 190 kV.

Table 1:  $\text{Al}_2\text{O}_3$  and  $\text{SiO}_2$  Comparisons

Material	Index $n$	Cher. Thresh.	TIR Thresh.
$\text{SiO}_2$	1.46	190 kV	987 kV
$\text{Al}_2\text{O}_3$	1.77	108 kV	190 kV

Optical comparisons between the two materials at various temporal locations are shown in Fig. 3. Conditions were kept nearly identical for both diagnostics: 7.5 mm cathode, 30 ns imaging gate with a constant gain, 108 mm viewing diameter, material thickness of 1 mm, and current and voltage levels within a reasonable level of deviation. There is an obvious difference in intensity levels between the two materials, further demonstrated in Fig. 4. The images taken from 220-250 ns correspond to a beam energy slightly below the 190 kV threshold. At this temporal location, the  $\text{SiO}_2$  image intensity decreases due to the beam energy dropping below the Cherenkov radiation threshold.

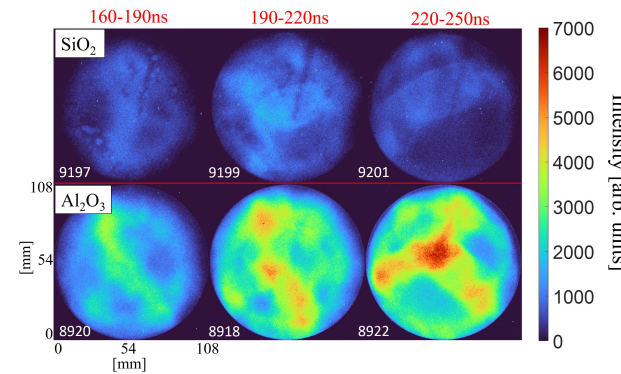


Figure 3: Image comparisons for  $\text{SiO}_2$  (top) and  $\text{Al}_2\text{O}_3$  (bottom) throughout the head of the voltage pulse.

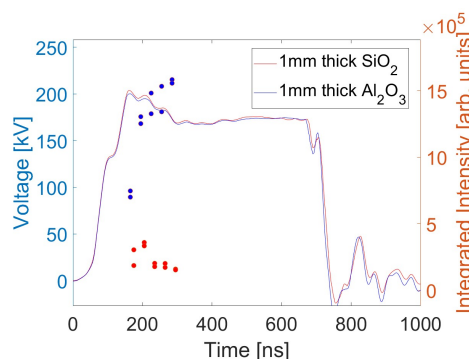


Figure 4: The voltage waveforms corresponding to Fig. 3. Results were produced with a 7.5 mm-diameter cathode.

## MCNP6® MODELING

Optimal material configurations are predicted and tested utilizing MCNP6® [8]. Models account for Cherenkov emission, electron scatter, and bremsstrahlung X-ray production. The simplistic model is a pencil beam of electrons at a defined energy colliding with a given diagnostic configuration. Cherenkov photon production is enabled and secondary electron production is turned off. Even with a simplified model, predictions can be made on whether the experimental distribution is due to electron scatter, effects from Cherenkov radiation, or due to underlying beam physics not represented in the model (i.e. space charge, edge emission, emittance growth, and excess emission).

The photon flux for the simplified model is shown in Fig. 5. The beam energy is 250 kV and is colliding with 1 mm-thick  $\text{SiO}_2$  located at the origin. Photon production is primarily a result of bremsstrahlung and Cherenkov radiation. Though there are some irregularities, the distribution at  $z = 20$  mm, approximately 20 mm off the surface of the diagnostic, is mostly uniform and does not exhibit patterns seen in Fig. 3. The patterns shown in Fig. 3 are a result of excess edge emission produced with the 7.5 mm cathode that the model does not take into account. Future improvements will be made on the present model to better represent experiments performed on the CTS.

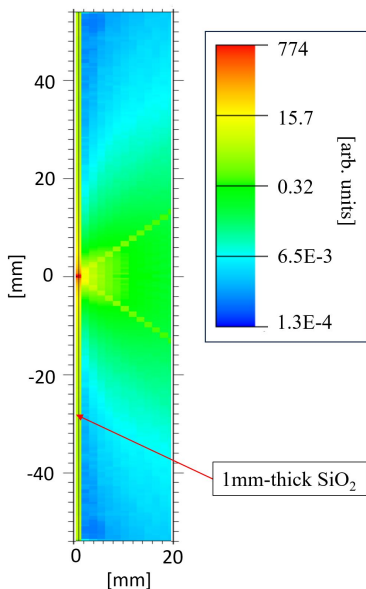


Figure 5: Photon flux for  $\text{SiO}_2$  diagnostic for  $V=250$  kV.

## CONCLUSIONS AND FUTURE WORK

Due to the capabilities of the CTS, produced electron beams are in the sub-relativistic regime presenting a myriad of challenges in measuring current density on a diagnostic screen. Present results demonstrate that electron scatter plays a large role in constraining measurements. Additional difficulty comes from Cherenkov emission and total internal

reflection. It has been experimentally demonstrated that materials with varying  $Z$  and index of refraction  $n$  produce distributions with differing intensity, shot variability, and reliability.

Future efforts include further testing of Cherenkov emitters with a focus on materials with  $n$  ranging from 1.5 - 1.75. Emitter size plays a large role in emission patterns and thus the current density distributions. Smaller cathodes, such as the 7.5 mm diameter cathode, are subject to large amounts of edge emission as the triple point is fully exposed. Preliminary measurements have been taken with a 25 mm diameter velvet cathode and show a dramatic change in current density imaging. Details on these results will be published elsewhere.

## ACKNOWLEDGEMENTS

The authors would like to thank LANL's Monte Carlo Codes group for their advice and guidance with MCNP6® simulation development, with special thanks to Jeff Bull and Colin Josey. We would also like to thank Mike Jaworski for his assistance with the computational modeling.

## REFERENCES

- [1] S. Russell *et al.*, "First observation of elliptical sheet beam formation with an asymmetric solenoid lens," *Phys. Rev. ST Accel. Beams*, vol. 8, p. 080401, 2005. doi:10.1103/PhysRevSTAB.8.080401
- [2] R. B. Fiorito and D. W. Rule, "Optical transition radiation beam emittance diagnostics," in *AIP Conference Proceedings*, vol. 319, 1994. doi:10.1063/1.46965
- [3] M. Butram and R. Hamil, "Cherenkov Light as a Current Density Diagnostic for Large Area, Repeatively Pulsed Electron Beams," in *Proc. PAC'83*, Santa Fe, NM, USA, Mar. 1983, pp. 2216–2219.
- [4] K. Pepitone, "Etude de la production, de la propagation et de la focalisation d'un faisceau d'électrons impulsions intense [Study of the production, propagation and focusing of an intense pulsed electron beam]. Physique des plasmas [physics.plasm-ph]," Ph.D. dissertation, Universite de Bordeaux, 2014, Francais.
- [5] K. Pepitone, J. Gardelle, and P. Modin, "Optimizing the emission, propagation, and focusing of an intense electron beam," *J. Appl. Phys.*, vol. 117, p. 183301, 2015. doi:10.1063/1.4919832
- [6] M. R. Howard, J. E. Coleman, and S. M. Lidia, "Studying the Emission Characteristics of Field Emission Cathodes with Various Geometries," in *Proc. NAPAC'22*, Albuquerque, NM, USA, 2022, pp. 226–228. doi:10.18429/JACoW-NAPAC2022-MOPA79
- [7] Teledyne Princeton Instruments, <http://www.princetoninstruments.com/products/imcam/pimax/>.
- [8] J. A. Kulesza *et al.*, *MCNP® Code Version 6.3.0 Theory & User Manual*, Available at [https://mcnp.lanl.gov/pdf\\_files/TechReport\\_2022\\_LANL\\_LA-UR-22-30006Rev.1\\_KuleszaAdamsEtAl.pdf](https://mcnp.lanl.gov/pdf_files/TechReport_2022_LANL_LA-UR-22-30006Rev.1_KuleszaAdamsEtAl.pdf), Los Alamos National Laboratory, 2022.